Exp Fluids (2007) 42:863–869
DOI 10.1007/s00348-007-0275-5

RESEARCH ARTICLE

Visualization of a supersonic air micro jet by methods of dual-hologram interferometry

J. G. Velásquez-Aguilar · G. Toker · A. Zamudio-Lara · M. Arias-Estrada

Received: 8 July 2006 / Revised: 30 January 2007 / Accepted: 2 February 2007 / Published online: 9 May 2007

Abstract Visualization and investigation of supersonic air micro jets (SAMJ) as weak phase objects present serious problems when done through classical visualizing methods. Usage of advanced holographic interference techniques would make the study and evaluation of characteristic densities, density gradients and jet's structure (weak shocks followed by expansion waves) more successful. It should be remarked, that the applications of Mach-Zehnder (reference) and shear dual-hologram techniques, which were performed in earlier works, have been done separately and have a demonstrative character. In the present paper, the authors have tried to apply both the dual-hologram techniques, simultaneously. This approach makes it possible to measure the same phase object under study by reference beam and shear interference techniques using only Mach-Zehnder holograms. Finally, experimental data obtained from both the techniques were numerically compared and found to be more applicable. It was first experimentally shown that sensitivity of shear interference approach during evaluations of radial component of density gradients in a micro jet can be enhanced by using the technique of re-recording holograms. The effect of fast transition to a transonic regime accompanied by expansion and later on with disintegration of a jet was observed and jet's densities and radii in transition region were evaluated. As a whole, method of co-joint application of reference beam and shear dual-hologram interferometry has shown its self-descriptiveness, flexibility and utility for optical diagnostics of a weak gas dynamic micro object, the supersonic air micro jet.

J. G. Velásquez-Aguilar · G. Toker (✉) ·
A. Zamudio-Lara
Centro de Investigación en Ingenieria y Ciencias Aplicadas/
UAEM, 62209 Cuernavaca, Morelos, Mexico
e-mail: toker@buzon.uaem.mx

J. G. Velásquez-Aguilar
e-mail: jgpeva@uaem.mx

A. Zamudio-Lara
e-mail: azamudio@uaem.mx

M. Arias-Estrada
Instituto Nacional de Astrofisica, Optica y Electronica,
72000 Puebla, Puebla, Mexico
e-mail: ariasmo@inaoep.mx

1 Introduction

In recent years, there has been considerable research in the field of dynamics of supersonic air micro jets (SAMJ) due to their potential use in applications such as micro-propulsion, cooling of MEMS components and fine particle deposition and removal.

Experimental studies of supersonic micro jets were performed usually by applying standard gas dynamic techniques (Scroggs and Settles 1996; Phalnikar et al. 2001). Investigations of weak gas dynamic transparent micro objects, such as SAMJ, by applying standard flow field visualizing techniques present a complicated problem. First of all, it concerns small geometrical sizes of a jet, relatively low sensitivity of the techniques as well as adequacy of the acquired optical information. Although in literature, the numerous experiments have been described, which were performed with the help of the micro-Schlieren system with a large magnification (see for example Phalnikar et al. 2001), qualitative analysis shows that studying SAMJ by different ''fringe'' techniques is more preferable because interferometry is a more advanced technique due

to its powerfulness, flexibility and numerical character. Most powerful and applicable interference techniques are holographic ones (Toker at al. 1997; Gopalan 2001; Mizukaki et al. 2000) since they possess remarkable advantages over classical approaches during study of gas dynamic micro objects.

A SAMJ with a diameter of 1.3 mm already has been studied by different methods of dual-hologram interferometry (Toker et al. 1995, 1997 Toker and Levin 1997) separately and they had a demonstrative character. It was shown that this micro object can be visualized and studied by using low spatial frequency holograms recorded on a 35 mm photographic film. Earlier gas dynamic macro objects have been successfully investigated by using low spatial frequency holograms (Tanner 1966).

In the present paper, the authors have tried to apply both the dual-hologram techniques, simultaneously. It makes possible to measure the same phase object by reference-beam and shear techniques using only three Mach-Zehnder holograms: one comparison hologram and two identical signal ones. The comparison and one of the signal holograms might be used in a reconstruction scheme in order to generate a series of reference beams reconstructed interferograms including interferograms with enhanced sensitivity (Toker et al. 1997) with different widths of the fringes. The two identical signal holograms might be used for generating a series of reconstructed shear interferograms with different lateral shifts.

Holograms with spatial frequencies 20–50 mm^{-1} have been successfully recorded on the photo material KODAK 100 Tmax (ISO 100). A thin amplitude hologram having the spatial resolution ~50 mm^{-1} demonstrates (Collier et al. 1971) linear resolution of the order of 30 microns, which allows studying SAMJ with diameters of the order of 0.3 mm and using optical imaging and reconstruction schemes achromats.

A SAMJ was generated by using the cylindrical nozzle with internal diameter of 1.0 and outer diameter of 2.0 mm. For producing a SAMJ, a compressed air pipe line with stagnation pressure $p_0 = 7$ atm was used. Expansion ratio $p_e/p_a = 3.7$ is calculated taking into account ambient pressure $p_a = 1$ atmosphere and the ratio $p_e = 0.528\ p_0$, where p_e is exit pressure. *Re* number for the air jet of 1 mm diameter is determined as $Re = 2.27 \times 10^5$.

2 Visualizing and studying a micro jet by dual-hologram methods

Low spatial frequency reference beam holograms of a jet were recorded by applying a scheme of Mach-Zehnder interferometer based on two beam-splitting cubes. A jet was photographed in the light of a CW helium-neon 632.8 nm@10 mW gas laser. The spatial frequency of holograms did not exceed 50 mm^{-1}; therefore the holograms could be easily recorded on 35 mm panchromatic KODAK Tmax 100 and 125 PX photo films having a resolving power of 100 mm^{-1}. In order to re-record secondary holograms on the same photo film, the master ones were recorded preliminary with the reduced spatial frequencies 15–20 mm^{-1}. The size of a picture area is 24×36 mm^2. Rotating output beam-splitting cube over its vertical axis allows controlling a spatial frequency of holograms with vertically directed fringes. A SAMJ was focused by using a collimator consisting of two achromats into the plane of a photo film with magnification of 3.5X.

It should be specially remarked that all recorded amplitude holograms, having up to a certain extent of enhanced optical densities, were bleached. It is known that phase holograms have notably higher diffraction efficiency in comparison with amplitude ones (Collier et al. 1971). Fortunately the above-mentioned photo films are characterized with a relatively low effect of scattering after bleaching. By virtue of this phase, holograms are more preferable in schemes of reconstruction.

Recorded reference beam signal and comparison holograms or two signal holograms in the case of shear approach were placed in a dual hologram holder for the purpose of reconstructing reference beam or shear interferograms (Toker et al. 1995). After that, the holograms were illuminated by a parallel beam behind a collimating achromat in the reconstruction scheme. A jet was sharply focused into the plane of the photo film inside a photo camera (without its attached lens) by the collimator consisting of two achromats. During the process of reconstruction, a stop diaphragm located in the region of co-focus collimating achromats, which build a focused image of the photo film, produces an optical selecting only plus (or minus) first diffraction order; other orders are stopped.

2.1 Recording and reconstruction of reference beam holograms

In Fig. 1a, an out-of-focus shadow image confirms the supersonic character of a micro jet. It is seen that the flow consists of a periodic system of ‘‘cells’’, the structure with successive shocks and expansion waves were observed earlier by Toker et al. (1997); Phalnikar et al. (2001); Scroggs and Settles (1996). The jet can be clearly observed as far as 5 diameters downstream; after that becomes the process of expansion and disintegrating. Typical reconstructed reference beam interferograms are presented in Fig. 1b–d. The ‘‘cell’’ structure is also observed on the

infinite width fringe interferogram in Fig. 1b, where the process of expansion is clearly observed.

It must be commented that a SAMJ is also the gas dynamic system with weak shock phenomena where Mach numbers of shocks are only slightly larger than unity. The fast process of expansion shows effective transition of supersonic regime in transonic one and finally the disintegration of a SAMJ. The expansion process is accompanied by decreasing compression of air in a jet at longer distances downstream and blurring ''cells'' on the interferogram in Fig. 1b.

Taking into account the radial symmetry of a jet, radial density distributions were calculated on the basis of an inversion scheme of discrete annular elements, described in detail by Vest (1979). The finite width fringe interferograms in Fig. 1c, d demonstrate two different types of radial density distribution in shocks and expansion waves (Toker et al. 1997). Fringe shifts in a jet are relatively small: 0.2–0.3, therefore the errors of measurements of radial density distributions could be significant. The standard accuracy of fringe shift measurements is 0.1 of a fringe. The supreme value does not exceed 0.05. Thus, without enhancing sensitivity of the interference technique a radial density distribution could not be evaluated with accuracy better than ~20%.

In the case of the reference-beam interferograms (Fig. 1b–d) fringe shifts for certain distinctive changes of radial density of air:

$$\Delta\Phi(x) = 2\int_r^R \frac{[n(r) - n_a]rdr}{(r^2 - x^2)^{1/2}} = N\lambda, \qquad (1)$$

where $\Delta\Phi$ is the optical path length difference; λ is the laser wavelength, N is fringe shift, $n(r)$ is radial distribution of the index of refraction of air (Vest 1979).

2.2 Lateral shear reconstructed interferograms

Lateral shear interferograms were reconstructed from two identical signal Mach-Zehnder holograms as follows; the two holograms are placed in a dual hologram holder, a series of reconstructed shear interferograms can be recorded with different shifts and widths of interference fringes. The shifts depend upon amplitudes of transverse deposition of the two Mach-Zehnder holograms. A series of reconstructed lateral shear interferograms with different shears in horizontal as well as in vertical direction are presented in Fig. 2. The interferograms were reconstructed from the holograms having vertical system of fringes of the same spatial frequencies. In order to arrange vertical system of interference fringes, the two Mach-Zehnder signal holograms should also be recorded with vertical system of fringes but with a bit different spatial frequencies. The technique was suggested for the first time by Toker et al. (1995).

Notice that the behavior of fringes in shear interferograms is characterized by odd (anti-symmetric) functions, whereas in reference-beam interferogram, by even functions. In shear interferograms in Fig. 2a–b, a fringe pattern is formed by the interference of two identical wave fronts, which is reconstructed from the two Mach-Zehnder holograms and horizontally displaced with respect to each other at lateral shear s: $\Delta\varphi = \varphi(x–s, y) – \varphi(x, y)$, where φ is phase of a wave front. The two reconstructed wave fronts give in the direction of the plus first (minus first) order an interference pattern with intensity $2[1 + \cos(\varphi_s\text{-}\varphi)+2\pi f_y y)$, where f_y is spatial frequency of the interference pattern.

Physical interpretation of fringe shifts in shear interferograms is the following. From the viewpoint of optical diagnostics at a small lateral shift of wave fronts, they determine projections of angle of deflection of the diagnostic beam. From gas dynamic point of view, they can be

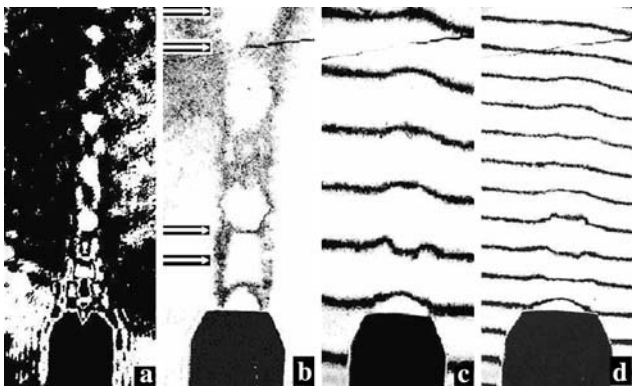

Fig. 1 Out-of-focus shadowgraph (**a**) and reconstructed reference beam interferograms (**b–d**). **b** Infinite width fringe; **c**, **d** finite width fringe interferograms. Outer diameter of nozzle is 2 mm; internal diameter is 1 mm. Time exposure 1×10^{-3}s

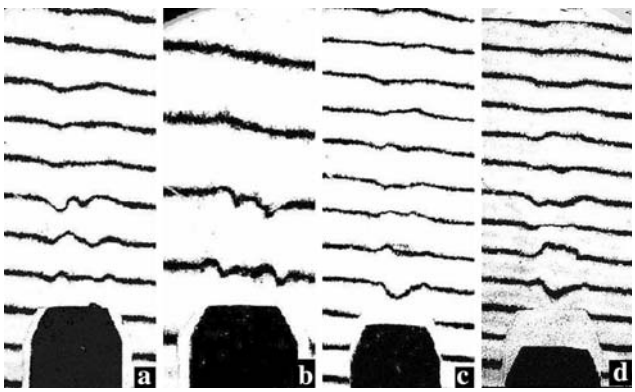

Fig. 2 Reconstructed dual hologram shear interferograms (**a–d**): finite width fringe interferograms. Horizontal shears, **a** 0.18, **b** 0.24 mm; vertical shears, **c** 0.36, **d** 0.68 mm

interpreted as the radial component of density gradients as long as lateral fringe shifts were performed in the radial direction (Merzkirch 1987).

The reconstructed shear interferograms manifest largest radial air density gradients in the vicinity of the boundary of a jet and undisturbed air dragged into flow motion. Due to the co-joint interference approach they may give qualitative and (partially) quantitative supplement to the data obtained by using reference beam with information on the sign and value of radial component of density gradients, that will be shown below.

2.3 Sensitivity enhancement of dual hologram interference measurements

In order to diminish errors and increase the calculating accuracy of the air density and density gradient distributions in a jet, two reference beam signal holograms, as the master ones, were overwritten in the second diffraction orders by applying the holographic technique discussed by Toker et al. (1997). Correspondent comparison master hologram was also re-recorded in second symmetrical orders. Toward this end, a specific two hole stop diaphragm is used, which selects only plus and minus second diffraction orders; others are stopped. The two secondary holograms, signal and comparison were placed in a dual hologram holder for the purpose of generating reconstructed reference beam interferograms in plus (or minus) first orders with enhanced sensitivity. In the case of rewriting plus and minus second orders, the interference measurements are increased by factor of 4 (see the reconstructed interferograms Fig. 3a, b.

The two Mach-Zehnder signal secondary holograms, one of which had been used for reconstruction of the interferogram, Fig. 3b, were used for generating a series of shear interferograms with enhanced sensitivity. These signal reference-beam holograms have been located in a dual hologram holder and a series of interferograms with sensitivity enlarged by factor of 4 were reconstructed with different horizontal and vertical shifts. Two of these interferograms with horizontal shifts are demonstrated in Fig. 3c, d.

2.4 Computations of radial density distributions

Radial density distributions were computed by using the interferograms, Fig. 3b and Fig. 1c, d. The densities were numerically calculated in two cross-sections located at distances 0.94 and 1.38 mm from the cut of a nozzle, as shown in Fig. 1b by the arrows. The cross-sections correspond to an expansion wave at a distance of 0.94 mm and a shock structure (1.38 mm) from the nozzle. The results of computer calculations are imaged in Fig. 4a. Early radial density distributions for a jet with diameter 1.3 mm were calculated by Toker at al. (1997). It can be seen in Fig. 4a, that maximal compression in the case of a weak shock is realized in the center (plot 1) of a jet and achieves the value of $\rho_c/\rho_a = 1.6$, where ρ_c is air density in the center of a jet. As to the radial distribution (plot 2) for an expansion wave, the jet with diameter 1.0 mm is characterized with larger gradients than for the jet with diameter 1.3 mm in the vicinity of the boundary of the jet and undisturbed air.

Radial density distributions in the transition region are also convenient to calculate by using the interferogram imaged in Fig. 3b. Densities were computed for two cross-sections: 4.44 and 5.40 mm from cut of the nozzle. The results are presented in Fig. 4b. A jet enlarges its size in radial direction for these cross-sections: new radii are 1.28 and 1.44 mm, correspondingly. At the same time, compression in the center of a jet drops significantly, diminishing to the factor of $\rho_c/\rho_a = 1.26$ and 1.16. Early quantitative measurements providing jet decay and spreading rates were obtained via pressure surveys using micro-pitot probes by Scroggs and Settles (1996); Phalnikar et al. (2001).

2.5 Computations of radial density gradient distributions and numerical comparison of the techniques

As it was already noticed that reference beam interferograms with finite width fringes may be used for definite calculating of radial density distributions, like for instance, in the case of shear interferograms imaged in Fig. 2a, b and Fig. 3c, d, fringe shifts can be interpreted as the radial component of gradients of air density, only if we take into account the two following conditions. The first one: radial gradients must be normalized by the amplitude of the shift. It connects with the fact that sensitivity of shear measurements depends upon the amplitude of a lateral shear. The second condition is: it may be done only for lateral shifts smaller than an optimal one, when a contribution of second derivative in the function of radial gradients is negligibly small. Thus, the optimal shift is determined as a maximal possible shift, when distortions still are negligibly small.

Taking into account these conditions, let us try to compare numerical data for the radial component of density gradient obtained in two different ways. First one: the radial density distributions (Fig. 4a) for a weak shock and an expansion wave could be differentiated and the corresponding data for the radial component of density gradients can be found directly. Second one: data for the radial component of density gradients could be calculated from reconstructed shear interferograms, Fig. 2a, b and Fig. 3c, d at correspondent distance from cut of the nozzle. These

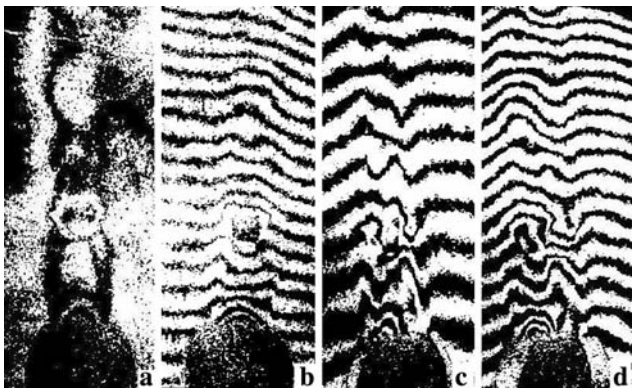

Fig. 3 Reconstructed reference beam and shear interferograms with sensitivity enhanced by factor of 4. Reference beam interferograms: **a** infinite width fringe; **b** finite width fringe interferograms. Shear interferograms: horizontal shifts, **c** 0.18; **d** 0.24 mm

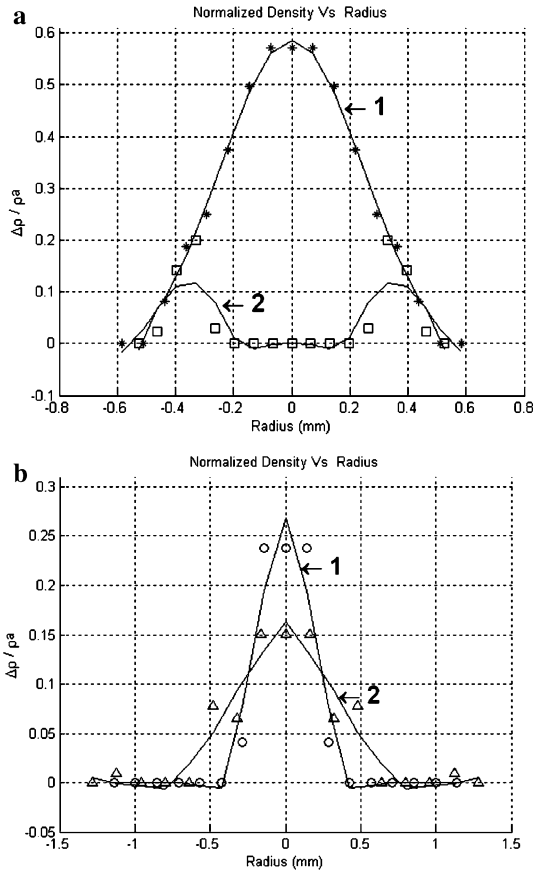

Fig. 4 Radial distributions of density in a jet for four cross-sections located at distances: **a** (*1*) 0.94, **a** (*2*) 1.38; **b** (*1*) 4.44, **b** (*2*) 5.4 mm from cut of the nozzle

interferograms were reconstructed with the two horizontal (radial) lateral shifts: 0.18 and 0.24 mm. The radial component of density gradients was also calculated by using the inversion scheme of discrete annular elements, described by Vest (1979). Interference data for fringe shifts were made symmetrical and smoothed over. As a result of this, an accuracy of measurements of gradients does not exceed 30%. The numerical comparison for a weak shock and an expansion wave is illustrated in Fig. 5a, b. Graphical comparison of numerical differentiation of the radial density distribution (Fig. 4a) with calculated data for interference pictures, Fig. 2a, b and Fig. 3c, d is shown in Fig. 5a. The optimal lateral radial shift was determined on the level ~0.1 mm. The calculated radial component gradient data were normalized in accordance with the shifts 0.18 and 0.24 mm. These graphs determine the situation in the case of a weak shock wave located approximately at a distance of 1.0 mm from the nozzle. The situation with an expansion wave is imaged in Fig. 5b. The corresponding radial component of density gradients was calculated at the distance of about 1.4 mm from the nozzle.

It is seen from the graphs in Fig. 5a, b that for shifts 0.18 and 0.24 mm exceeding the optimal shift s~0.1 mm, the radial components of density gradients look more smooth with local maximums with larger amplitudes and displaced to the center of a jet.

3 Conclusions

As a whole, method of dual-hologram interferometry by co-joint application of both the interference techniques showed its self-descriptiveness, flexibility and utility for optical diagnostics of such the weak gas dynamic micro object as a supersonic air micro jet. As a matter of fact, to generate all interferograms presented in Figs. 1–3, it was necessary to have three master holograms only: two identical signal holograms and one comparison. Note that in order to arrange vertical interference fringes (not shown in the figures) it requires two holograms with a bit of different spatial frequencies.

Holograms reconstructed in a dual hologram holder make the generation of an interference fringe, just through the region of interest, [see also Hannah and King Jr (1977)]. In our case at some fixed distance from top of the nozzle, the fringe may cut traverse a weak shock or the center of an expansion wave.

If sensitivity of interference measurements is not enough it can be enlarged. The authors hope that a newly designed special reconstruction scheme, based on Mach-Zehnder interferometer, will make it possible to study a jet with a diameter of the order of 0.1 mm or lesser. In this case to provide higher linear resolution instead of achromats imaging objective lens optics must be used.

Usual 35 mm B&W photo films could be successfully used for visualizing and studying supersonic gas dynamic micro phenomena. Presently, literature analysis shows only

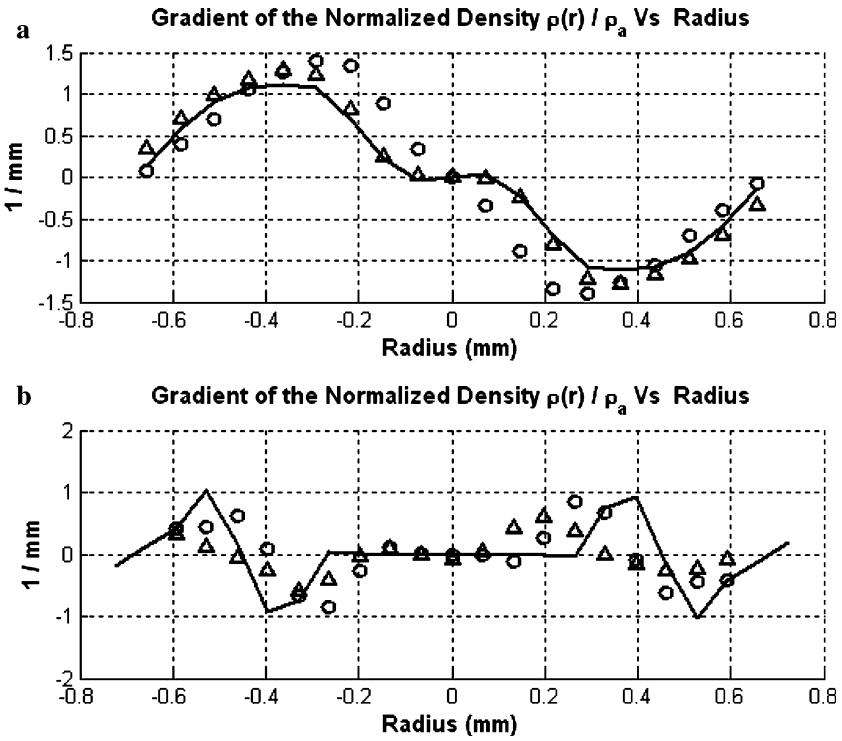

Fig. 5 Radial distributions of density gradient in a jet for four cross-sections located at distances: **a** ~1.0 (weak shock); **b** 1.4 mm (expansion wave) from cut of the nozzle. *Triangle* is shift 0.18 and *Circle* is 0.24 mm. The *solid line* represents the gradients of the normalized densities shown in Fig. 4a(1, 2)

a few articles, where authors apply holographic interferometry approach and none of them used photo materials, which require a wet photo processing. Digital imaging by using CCD/CMOS sensors is considered more attractive. The scientific age of the above-mentioned photo films is not over. The aperture 36×24 mm^2 is larger than most of the digital sensors. The spatial resolution is not worse and frequently better. The latter means that an optical system may image the micro object under test with better linear resolution or, in other words, may satisfactorily image the micro objects with smaller non-uniformities. The sensitivity is comparable or may be enhanced by using speedy photo films with ISO = 400, saving the resolution. Finally, the technique is applicable with small investments.

The observed fast gas dynamic expansion and further disintegration of a SAMJ could be explained in addition by low supersonic velocities, which are only slightly larger than unity in the vicinity of the nozzle's cut. It seems also that a jet having a smaller diameter showing a bit larger density gradients on the boundary of undisturbed air is affected more crucially by undisturbed air and disintegrates more rapidly.

The most remarkable feature of this article is the joint application of both the interference techniques. In the suggested approach we use, for producing reconstructed reference-beam and shear interferograms, the same signal holograms, therefore the same gas dynamic object is subjected to testing. This circumstance is of high importance in the case of using pulsed laser systems for studying transient gas dynamic objects or for turbulent interference measurements. Finally, we can conclude that to get a series of reference-beam and shear reconstructed interferograms of the same object requires only three Mach-Zehnder holograms: two identical signal ones and another comparison hologram. The signal holograms (amplitude or phase) can be successfully obtained by methods of contact photo or optical coping from one master hologram, taking into account its low spatial frequency.

Acknowledgments The authors would like to express their appreciation to Drs. J. G. Gonzalez-Rodriguez, Alberto Alvares Gallegos, V. Agarwal and Mr. D. P. Noyola for help. The authors would like to acknowledge Consejo Nacional de Ciencia y Tecnología (CONACYT-México), for the grant given to J. Guadalupe Velasquez Aguilar (Beca No. 130082). Declaration: The Experiments Comply with the current laws of Mexico.

References

Collier R, Burckhardt C, Lin L (1971) Optical holography. Academic, New York

Gopalan J (2001) Holographic interferometric observation of micro-shock wave and supersonic jet interactions (Invited Paper) 2001 fluids engineering division summer meeting, May 29, June 1, 2001, New Orleans, Louisiana

Hannah BW, King WL Jr (1977) Extensions of dual-plate holographic interferometry. AIAA J 15:725–727

Merzkirch W (1987) Flow visualization. Academic Press, Orlando

Mizukaki T, Takayama K, Kleine H (2000) Digital phase shift holographic interferometer for the visualization of shock wave

phenomen. In: 53rd Annual meeting of the division of fluid dynamics, November 19–21, 2000 Washington, DC
Phalnikar KA, Alvi FS, Shih C (2001) Behavior of free and impinging supersonic microjets. AIAA 2001–3047
Scroggs S, Settles G (1996) An experimental study of supersonic microjets, Exp Fluids 21(6):401–409
Tanner L (1966) Some applications of holography in fluid mechanics. J Scien Instrum 43:81–83
Toker G, Levin D (1997) Comprehensive optical diagnostics of complex flow fields. In: SPIE Conference #3110–81, 574–585
Toker G, Levin D, Stricker J (1995) Experimental investigation of super/hypersonic flow fields based on a new approach using holographic optical techniques. In: International congress on instrumentation in aerospace simulation facilities, 10.1–10.7
Toker G, Levin D, Stricker J (1997) Dual hologram technique with enhanced sensitivity for measurements of weak phase objects. Exp Fluids 22:354–357
Vest C (1979) Holographic interferometry. Wiley, New York